Fixed-Time Rigidity-Based Formation Maneuvering for Nonholonomic Multirobot Systems With Prescribed Performance

Ke Lu[®], Graduate Student Member, IEEE, Shi-Lu Dai[®], Member, IEEE, and Xu Jin[®], Member, IEEE

Abstract—This article presents rigidity-based formation maneuvering for a group of nonholonomic mobile robots subject to limited sensing capability, where the performance bounds are introduced to constrain the distance and angle errors. The timevarying and asymmetric performance constraints can prescribe the transient and steady-state performance of the closed-loop systems, which further specify collision avoidance and connectivity maintenance among neighboring robots and avoid the controller singularity issue. To satisfy the constraint requirements and fixed-time convergence, universal barrier Lyapunov functions are incorporated with control design such that angle errors are fixed-time stable and distance errors can converge to a small neighborhood around zero in fixed time. Under the proposed control protocol, all robots can track the desired timevarying velocity while generating and maintaining the predefined formation defined by a minimally and infinitesimally rigid graph. Simulation and experiment studies are carried out to illustrate the effectiveness of the proposed control protocol.

Index Terms—Collision avoidance, connectivity maintenance, formation maneuvering, nonholonomic mobile robots, prescribed performance, rigidity graph.

I. INTRODUCTION

OOPERATIVE control of multiagent systems has received considerable research interest in the fields of control and robotics during the past decades. Many complex tasks are accomplished efficiently by the cooperation of multiple agents, such as cooperative coverage, exploration, entrapment [1], etc. Control problems in multiagent

Manuscript received 4 March 2022; revised 30 May 2022 and 4 November 2022; accepted 17 November 2022. Date of publication 16 December 2022; date of current version 18 March 2024. The work of Ke Lu and Shi-Lu Dai was supported in part by the Southern Marine Science and Engineering Guangdong Laboratory (Zhuhai) under Grant SML2022SP101; in part by the National Natural Science Foundation of China under Grant 61973129, Grant 42227901, Grant 62273156, and Grant 62073090; and in part by the Guangdong Basic and Applied Basic Research Foundation under Grant 2021A1515012004. The work of Xu Jin was supported in part by the United States National Science Foundation under Grant 2131802. This article was recommended by Associate Editor P. Shi. (Corresponding author: Shi-Lu Dai.)

Ke Lu and Shi-Lu Dai are with the School of Automation Science and Engineering, Key Laboratory of Autonomous Systems and Networked Control, Ministry of Education, South China University of Technology, Guangzhou 510641, China, and also with the Southern Marine Science and Engineering Guangdong Laboratory (Zhuhai), Zhuhai 519000, China (e-mail: lukenanlin@163.com; audaisl@scut.edu.cn).

Xu Jin is with the Department of Mechanical and Aerospace Engineering, University of Kentucky, Lexington, KY 40506 USA (e-mail: xu.jin@uky.edu). This article has supplementary material provided by the authors and color versions of one or more figures available at https://doi.org/10.1109/TCYB.2022.3226297.

Digital Object Identifier 10.1109/TCYB.2022.3226297

coordination can be typically categorized into formation stabilization [2]; formation tracking [3]; and formation maneuvering [4], [5]. Formation stabilization refers to the generation of a stationary geometrical shape, while formation tracking requires multiple agents to set up a desired formation geometry and move along a reference trajectory. Formation maneuvering corresponds to simultaneous shape stabilization and tracking the desired reference velocity [6].

In the context of multiagent systems, the rigid graph theory is an important tool to describe the formation geometry in rigidity formation control, where the desired formation geometry is generated by controlling the interagent distances [7] and interagent bearings [8], [9], [10]. However, most existing rigidity-based algorithms in the literature can only be applied to solve the formation control problem of multiagent systems modeled by single-integrator or double-integrator kinematics. The nonholonomic kinematics is a more realistic model for wheeled mobile robots in formation control [11], [12], [13], [14], which makes rigidity-based control design more challenging. The distance-based control framework has been recently applied to nonholonomic kinematic agents [15], in which the nonholonomic systems are converted into singleintegrator-like systems that include a multiplicative matrix dependent on the heading angle errors of the agents.

There are several significant issues associated with formation maneuvering problems of nonholonomic multirobot systems. The first one is the safety problem, which may deteriorate system performance or even result in system failure. The safe navigation of robot swarms usually requires that interrobot collision never occurs, which relates to collision-avoidance problem in [16], [17], [18], and [19]. In addition to collisions, the limited sensing capability is another safe hazard. The onboard sensors equipped with robots can only detect their neighbors that stay within a certain sensing range; otherwise, the information interaction among robots may be broken, which results in the connectivity maintenance problem [20], [21], [22], [23]. To deal with such a safety problem, artificial potential functions [17], [24] and constrained control systems [25], [26] have been developed. In [17] and [24], a repulsive vector field is constructed around the agents and the potential function is equal to zero when the desired formation is achieved, and grows to infinity when any collision occurs or network connectivity is broken. In [25] and [26], interagent distances are enforced to evolve within a certain range such that the safety requirement is never violated during the formation motion.

2168-2267 © 2022 IEEE. Personal use is permitted, but republication/redistribution requires IEEE permission. See https://www.ieee.org/publications/rights/index.html for more information.

The second challenging issue relates to the performance of formation maneuvering systems including transient and steady-state performance, and convergence speed. Transient and steady-state behaviors are important performance specifications for a control system. A prescribed performance control (PPC) methodology [27] can guarantee the predefined transient and steady-state performance of output tracking errors by enforcing the given performance requirements in control design. Without depending on the trial-and-error method, the PPC methodology can guarantee that neighborhood errors converge to predefined residual sets, while the convergence rates of neighborhood errors are faster than the given values and the maximum overshoots are less than the given constants. Due to its remarkable properties, the PPC methodology [27] has been applied in the designs of fuzzy control [28], synchronization control [29], and formation control [25]. Recently, the PPC methodology is employed to develop a robust distance-based formation control with guaranteed transient performance, connectivity maintenance, and collision avoidance among neighboring agents [26]. Another performance specification is the settling time which characterizes the convergence rate of a control system [30], [31]. The fixed-time stability studied in [32] can provide guaranteed convergence time irrelevant to initial conditions which are unavailable a priori, which is extended to multiagent systems [33], [34], [35].

For constrained systems, any violation of constraint requirements may lead to unsatisfactory transient performance or system failure. To address the constraint problems, a barrier function, which grows to infinity whenever its argument approaches the constraint boundary, is introduced in constructing Lyapunov functions. Moreover, the barrier Lyapunov function can also be utilized to handle performance constraints for multiagent control systems, whereas the transient constraint problems are not discussed in the potential-functionbased control literature [17], [24]. The barrier functions, including logarithmic [36] and tan-type barrier functions [37], are applied to control systems with output/state constrains. Recently, a novel universal barrier function has been developed in [38], which can tackle both output-constrained and unconstrained nonlinear systems. How to address the safety and performance constraint requirements for nonholonomic multirobot systems under the distance-based framework is an important research topic that still remains to be developed.

This article presents fixed-time rigidity-based formation maneuvering for a group of nonholonomic mobile robots under the distance-based control framework, where the system performance and the safety requirement among neighboring robots are considered. Different from the leader-follower formation architecture studied in [3], [16], and [39], in which the communication graph is a simple directed spanning tree and each follower is only able to handle the constraint requirements from one leader, the presented formation maneuvering considers a minimally and infinitesimally rigid formation graph in which the communication graph is undirected and connected, and each robot is able to deal with the constraint requirements from more than one neighboring robots. The rigidity-based maneuvering problem for nonholonomic agents has been addressed in [15], where input transformation is

applied for the multiagent system. However, the settling time and the constraint requirements from safety and performance are not taken into account. Finite- and fixed-time controls of multiagent systems have been studied in [40], [41], and [42], but the transient responses or interagent constraints are not fully considered. Compared with control design for unconstrained systems or handling constraints between a pair of leader and follower, our approach that can deal with constraints among neighboring robots with the concern of the system performance is more challenging. The technical difficulties mainly stem from that: 1) although the modified input transformation can work for multiagent systems with prescribed performance, the singularity issue arises in control design; 2) the control design for each robot is expected to address constraints from its neighbors, and the stability analysis of barrier Lyapunov functions is more complex than that of the conventional quadratic form; and 3) the fixed-time control for system performance improvement is further addressed. The main contributions are summarized as follows.

- A fixed-time rigidity-based formation maneuvering protocol is presented for nonholonomic mobile robots, where the robots can track the desired time-varying velocity while converging to the desired shape defined by a minimally and infinitesimally rigid graph. With the consideration of a fixed-time control methodology, the angle errors are fixed-time stable, and the distance errors can converge into a small neighborhood around zero in fixed time and then asymptotically converge to the origin.
- 2) The safe navigation and limited sensing capability are considered during the entire formation motion, in which performance constraints are imposed on distance errors to satisfy the prescribed transient and steady-state performance, and further ensure the collision avoidance and connectivity maintenance among neighboring robots
- 3) The universal barrier function is incorporated with control design to deal with the constraint requirements and fixed-time convergence, and the singularity-free-constrained control design is guaranteed in the distance-based formation maneuvering framework.

II. PRELIMINARIES

A. Rigid Graph Theory

An undirected graph with n vertices and l edges is defined as $\mathcal{G} \triangleq (\mathcal{V}, \mathcal{E})$ where $\mathcal{V} = \{1, 2, \ldots, n\}$ is the set of vertices and $\mathcal{E} \subset \mathcal{V} \times \mathcal{V}$ is the set of undirected edges that connect two different nodes. If a node pair $(i,j) \in \mathcal{E}$, then so is (j,i). The set of neighbors of vertex i is defined as $\mathcal{N}_i(\mathcal{E}) = \{j \in \mathcal{V} | (i,j) \in \mathcal{E}\}$. Let $p_i \in \mathbb{R}^2$ denote the coordinate of vertex i, then a framework is defined as $\mathcal{F} \triangleq (\mathcal{G},p)$ where p is the stacked vector $p = [p_1^T,\ldots,p_n^T]^T \in \mathbb{R}^{2n}$. Based on the arbitrary ordering edges, an edge function $\Phi: \mathbb{R}^{2n} \to \mathbb{R}^l$ associated with (\mathcal{G},p) is given by

$$\Phi(p) = \left[, \dots, ||p_i - p_j||^2, \dots, \right]^T, \quad (i, j) \in \mathcal{E}$$
 (1)

where its kth element $||p_i - p_i||$ corresponds to the kth edge in \mathcal{E} connecting the *i*th and *j*th vertices. The rigidity matrix $R(p): \mathbb{R}^{2n} \to \mathbb{R}^{l \times 2n}$ of $\mathcal{F} = (\mathcal{G}, p)$ is defined as

$$R(p) = \frac{1}{2} \frac{\partial \Phi(p)}{\partial p} \tag{2}$$

where $\operatorname{rank}(R(p)) \leq 2n-3$ in \mathbb{R}^2 [43]. It should be noted that each row of rigidity matrix R(p) has the form $[\mathbf{0}_2^T, \ldots, (p_i - p_j)^T, \ldots, \mathbf{0}_2^T, \ldots, -(p_i - p_j)^T, \ldots, \mathbf{0}_2^T]$. Frameworks $\mathcal{F}_p = (\mathcal{G}, p)$ and $\mathcal{F}_{\hat{p}} = (\mathcal{G}, \hat{p})$ are equivalent if $\Phi(p) = \Phi(\hat{p})$, and are congruent if $||p_i - p_j|| = ||\hat{p}_i - \hat{p}_j|| \ \forall i, j \in \mathcal{V}$. A rigid framework is minimally rigid if no single interagent distance constraint can be removed without losing rigidity. A framework (\mathcal{G}, p) in \mathbb{R}^2 is minimally rigid if l = 2n - 3 [44]. A framework (\mathcal{G}, p) is infinitesimally rigid in \mathbb{R}^2 if rank(R(p)) = 2n - 3 [45]. Hence, if a framework is minimally and infinitesimally rigid, then the corresponding rigidity matrix has full row rank. An isometry of \mathbb{R}^2 is a bijective map $\mathcal{T}: \mathbb{R}^2 \to \mathbb{R}^2$ satisfying [46] $||x-y|| = ||\mathcal{T}(x) - \mathcal{T}(y)|| \quad \forall x, y \in \mathbb{R}^2$, where \mathcal{T} includes rotations and translations of the vector $x - y \in \mathbb{R}^2$. Two frameworks are regarded to be isomorphic in \mathbb{R}^2 if they are related by an isometry, and Iso(\mathcal{F}) represents the set of all isomorphic frameworks \mathcal{F} . Note that $\Phi(p)$ is invariant under isomorphic motions of the framework. If two infinitesimally rigid frameworks (\mathcal{G}, p) and (\mathcal{G}, \hat{p}) are equivalent but not congruent, then they are said to be ambiguous. The notation $Amb(\mathcal{F})$ denotes the set of all ambiguities of an infinitesimally rigid framework \mathcal{F} and its isometries. According to [44] and [47] (Theorem 3), it is reasonable to assume that all frameworks in $Amb(\mathcal{F})$ are infinitesimally rigid.

B. Useful Lemmas

Lemma 1 [48]: For any velocity $v \in \mathbb{R}^2$, it follows $R(p)(1_n \otimes v) = 0$, where 1_n is the $n \times 1$ vector of ones.

Lemma 2 [48]: Consider the function

$$\Psi(\mathcal{F}_p, \mathcal{F}_{\hat{p}}) = \sum_{(i,j) \in \mathcal{E}} (||p_i - p_j|| - ||\hat{p}_i - \hat{p}_j||)^2.$$

If \mathcal{F}_p is infinitesimally rigid and $\Psi(\mathcal{F}_p,\mathcal{F}_{\hat{p}}) \leq \delta$ where δ is a sufficiently small positive constant, then $\mathcal{F}_{\hat{p}}$ is also infinitesimally rigid.

Lemma 3 [49]: If the framework $\mathcal{F}_p = (\mathcal{G}, p)$ is minimally and infinitesimally rigid, then the matrix $R(p)R(p)^T$ is positive definite.

Lemma 4 [50]: If there exists a continuous radially unbounded and positive-definite function V(x) such that

$$\dot{V}(x) < -\alpha V^p(x) - \rho V^q(x)$$

for constants $\alpha > 0$, $\rho > 0$, p > 1, and 0 < q < 1, then the origin of the system is globally fixed-time stable and the settling time function T can be estimated by

$$T \le T_{\max} := \frac{1}{\alpha(p-1)} + \frac{1}{\rho(1-q)}.$$

Lemma 5 [35]: For $x_i > 0$, i = 1, ..., n, it follows:

$$\sum_{i=1}^{n} x_i^p \ge \left(\sum_{i=1}^{n} x_i\right)^p, \quad 0$$

$$\sum_{i=1}^{n} x_i^p \ge n^{1-p} \left(\sum_{i=1}^{n} x_i \right)^p, \quad p > 1.$$

III. PROBLEM STATEMENT

Consider a swarm of n nonholonomic mobile robots moving on the plane. The kinematics of the robot $i = \{1, 2, ..., n\}$, is described by

$$\dot{x}_i(t) = \cos \theta_i(t) v_i(t)
\dot{y}_i(t) = \sin \theta_i(t) v_i(t)
\dot{\theta}_i(t) = w_i(t)$$
(3)

where $p_i(t) = [x_i(t) \ y_i(t)]^T$ and $\theta_i(t)$ denote the position and heading angle of the robot i in the earth-fixed frame, respectively. $v_i(t)$ and $w_i(t)$ are linear and angular velocity control inputs.

Let the desired formation be represented by a minimally and infinitesimally rigid framework $\mathcal{F}^* = (\mathcal{G}^*, p^*)$, where $\mathcal{G}^*=(\mathcal{V}^*,\mathcal{E}^*)$, $\dim(\mathcal{V}^*)=n$, $\dim(\mathcal{E}^*)=l$, and $p^*=[p_1^{*T},\ldots,p_n^{*T}]^T\in\mathbb{R}^{2n}$. Then, the desired distance between the robot i and the robot j is given by

$$d_{\text{des},ij} = ||p_i^* - p_i^*||, \ (i,j) \in \mathcal{E}^*. \tag{4}$$

The actual formation shares the same framework \mathcal{F} = $(\mathcal{G}^*, p(t))$ with $p(t) = [p_1^T(t), \dots, p_n^T(t)]^T \in \mathbb{R}^{2n}$. The relative position $p_{ij}(t)$ and distance $d_{ij}(t)$ between the robot i and its neighboring robot j are given by

$$p_{ij}(t) = p_i(t) - p_j(t), \quad (i,j) \in \mathcal{E}^*$$
(5)

$$p_{ij}(t) = p_i(t) - p_j(t), \ (i,j) \in \mathcal{E}^*$$

$$d_{ij}(t) = \sqrt{\left(x_i(t) - x_j(t)\right)^2 + \left(y_i(t) - y_j(t)\right)^2}, \ (i,j) \in \mathcal{E}^*. (6)$$

Define the distance error

$$e_{ii}(t) = d_{ii}(t) - d_{\text{des }ii}, \ (i, j) \in \mathcal{E}^*$$
 (7)

where $d_{\text{des},ij}$ is the desired distance defined in (4).

A. Collision Avoidance

The safe navigation of the formation system requires that collisions among neighboring robots never occur. Accordingly, the constraint of safe distance \underline{d}_{ij} is imposed on the relative distance $d_{ij}(t)$ between the robot \vec{i} and its neighbor j to prevent collision, that is

$$0 < \underline{d}_{ij} < d_{ij}(t), \ (i,j) \in \mathcal{E}^* \quad \forall t \ge 0$$
 (8)

where \underline{d}_{ij} is the safe distance. Substituting (7) into (8) yields

$$d_{ii} - d_{\text{des},ij} < e_{ij}(t), \ (i,j) \in \mathcal{E}^* \quad \forall t \ge 0$$
 (9)

where $\underline{d}_{ij} < d_{\text{des},ij}$; otherwise, the desired formation is not feasible.

B. Connectivity Maintenance

Since the sensing capability is limited, it is necessary to ensure that each robot can reliably communicate with its neighbors during the formation motion. Thus, neighboring robots are required to remain within a limited sensing region, and this specification also imposes the constraint on the relative distance $d_{ii}(t)$ as follows:

$$0 < d_{ij}(t) < \bar{d}_{ij}, \ (i,j) \in \mathcal{E}^* \quad \forall t \ge 0$$
 (10)

where \bar{d}_{ij} is the maximum sensing range with $0 < \underline{d}_{ij} < \bar{d}_{ij}$. Substituting (7) into (10) yields

$$-d_{\text{des},ij} < e_{ij}(t) < \bar{d}_{ij} - d_{\text{des},ij}, \ (i,j) \in \mathcal{E}^* \quad \forall t \ge 0 \ \ (11)$$

where $d_{\text{des},ij} < \bar{d}_{ij}$; otherwise, the communication channel cannot be established. From (9) and (11), we obtain the following constraint:

$$-\underline{e}_{ij} < e_{ij}(t) < \overline{e}_{ij}, \ (i,j) \in \mathcal{E}^* \quad \forall t \ge 0$$
 (12)

where $\bar{e}_{ij} = \bar{d}_{ij} - d_{\text{des},ij}$ and $\underline{e}_{ii} = d_{\text{des},ij} - \underline{d}_{ii}$.

C. Infinitesimally Rigid Preservation

The requirement of a sufficiently small positive constant in Lemma 2 is a conservative estimate for how far \mathcal{F} can be from \mathcal{F}^* in order to remain infinitesimally rigid. A sufficient condition [26] is presented to establish infinitesimal rigidity of the actual formation \mathcal{F} based on the distance error bounds given in (12), which is restricted by

$$\sum_{(i,j)\in\mathcal{E}^*} |e_{ij}(t)| < \sum_{(i,j)\in\mathcal{E}^*} \max\left\{ |\underline{e}_{ij}(0)|, |\bar{e}_{ij}(0)| \right\} < \bar{\vartheta} \quad \forall t \ge 0$$

where $\bar{\vartheta} > 0$ is a sufficiently small constant. This implies that $|\underline{e}_{ij}(0)|$ and $|\bar{e}_{ij}(0)|$ are also sufficient small and, thus, it is reasonable to set $|\underline{e}_{ij}(0)| = |\bar{e}_{ij}(0)| = |e_{ij}(0)| + \mu$ with $\mu > 0$ being a sufficiently small constant. As a result, $e_{ij}(t)$ in (12) is also restricted by

$$-(|e_{ij}(0)| + \mu) < e_{ij}(t) < |e_{ij}(0)| + \mu. \tag{13}$$

Thus, it follows from (12) and (13) that:

$$-\underline{e}_{ii}^* < e_{ij}(t) < \bar{e}_{ii}^*, \ (i,j) \in \mathcal{E}^* \quad \forall t \ge 0$$
 (14)

where $\bar{e}_{ij}^* = \min\{\bar{d}_{ij} - d_{\text{des},ij}, |e_{ij}(0)| + \mu\}$ and $\underline{e}_{ij}^* = \min\{d_{\text{des},ij} - \underline{d}_{ij}, |e_{ij}(0)| + \mu\}.$

D. Performance Constraints

Define the following squared distance error:

$$\eta_{ij}(t) = d_{ij}^2(t) - d_{\text{des},ij}^2, \ (i,j) \in \mathcal{E}^*$$
(15)

which means from (7) that

$$\eta_{ij}(t) = e_{ij}(t) (e_{ij}(t) + 2d_{\text{des},ij}), (i,j) \in \mathcal{E}^*.$$
(16)

It is clear from (14) that

$$-\underline{\eta}_{ij} < \eta_{ij}(t) < \bar{\eta}_{ij}, \ (i,j) \in \mathcal{E}^*$$
 (17)

where $\bar{\eta}_{ij} = \bar{e}_{ij}^*(\bar{e}_{ij}^* + 2d_{\text{des},i})$ and $\underline{\eta}_{ij} = \underline{e}_{ij}^*(-\underline{e}_{ij}^* + 2d_{\text{des},i})$. Furthermore, we consider the following performance constraint imposed on $\eta_{ij}(t)$, that is:

$$-\underline{z}_{ij}\beta_{ij}(t) < \eta_{ij}(t) < \overline{z}_{ij}\beta_{ij}(t), \ (i,j) \in \mathcal{E}^* \quad \forall t \ge 0 \quad (18)$$

where $\underline{z}_{ij} > 0$ and $\overline{z}_{ij} > 0$ are design parameters, and $\beta_{ij}(t)$ is the design performance function given by

$$\beta_{ii}(t) = (\beta_{ii.0} - \beta_{ii.\infty})e^{-\gamma_{ij}t} + \beta_{ii.\infty}$$
 (19)

where $\beta_{ij,\infty}$ denotes the steady-state boundary with $0 < \beta_{ij,\infty} < \beta_{ij,0}$, and $\gamma_{ij} > 0$ is the decaying rate. In view of (18) and (19), at t = 0, $\eta_{ij}(t)$ has maximal bounds $-z_{ij}\beta_{ij}(0)$ and $\bar{z}_{ij}\beta_{ij}(0)$. Thus, we select $\underline{\eta}_{ij} = z_{ij}\beta_{ij}(0)$ and $\bar{\eta}_{ij} = \bar{z}_{ij}\beta_{ij}(0)$, respectively, which yields $\bar{z}_{ij} = \bar{e}_{ij}^*(\bar{e}_{ij}^* + 2d_{des,ij})/\beta_{ij,0}$ and $z_{ij} = \underline{e}_{ij}^*(-\underline{e}_{ij}^* + 2d_{des,ij})/\beta_{ij,0}$. In view of (16) and (18), the distance error is further restricted by following performance constraint:

$$-\underline{\alpha}_{ij}(t) < e_{ij}(t) < \bar{\alpha}_{ij}(t) \tag{20}$$

where $\bar{\alpha}_{ij}(t) = \sqrt{d_{\text{des},ij}^2 + \bar{z}_{ij}\beta_{ij}(t)} - d_{\text{des},ij}$ and $\underline{\alpha}_{ij}(t) = -\sqrt{d_{\text{des},ij}^2 - \underline{z}_{ij}\beta_{ij}(t)} + d_{\text{des},ij}$. Define the following error variable:

$$z_{ij}(t) = \frac{\eta_{ij}(t)}{\beta_{ii}(t)}, \quad (i,j) \in \mathcal{E}^* \quad \forall t \ge 0$$
 (21)

which converts the time-varying constraint (18) to the following time-invariant constraint:

$$-\underline{z}_{ij} < z_{ij}(t) < \overline{z}_{ij}, \ (i,j) \in \mathcal{E}^* \quad \forall t \ge 0.$$
 (22)

It is clear that if the constraint (22) is guaranteed by the designed controllers, the constraint (18) is satisfied, which indicates the satisfaction of (17) and (20). Then, the inequality (14) holds, which implies that the collision avoidance (9), connectivity maintenance (11), and infinitesimal rigidity (13) are guaranteed.

Assumption 1: At the initial time, the robot i is positioned at a given initial pose such that: 1) the robot i can establish communication channel and avoid collision with its neighboring robot j, that is, $\underline{d}_{ij} < d_{ij}(0) < \overline{d}_{ij}$, $(i,j) \in \mathcal{E}^*$ and 2) the initial angle error $\tilde{\theta}_i(0)$ does not violate the constraint $|\tilde{\theta}_i(0)| < \tilde{\theta}_{i,\max}$ with $\tilde{\theta}_{i,\max} \leq \pi/2$, where the angle error $\tilde{\theta}_i(t)$ is defined in (27).

Formation Maneuvering Objective: Under Assumption 1 and the minimally and infinitesimally rigid framework $\mathcal{F}^* = (\mathcal{G}^*, p^*)$, the formation maneuvering objective is to design the control laws $v_i(t)$ and $w_i(t)$, $i \in \mathcal{V}^*$, for system (3) such that:

- 1) the distance errors $e_{ij}(t)$, $(i, j) \in \mathcal{E}^*$ converge to a small neighborhood of zero in fixed settling time;
- 2) $\mathcal{F}(t) \to \operatorname{Iso}(\mathcal{F}^*)$ as $t \to \infty$ which is equivalent to $e_{ij}(t) \to 0$ as $t \to \infty$, $(i,j) \in \mathcal{E}^*$;
- 3) all robots move with the desired swarm velocity $v_0(t) \in \mathbb{R}^2$, that is, $\dot{p}_i(t) \to v_0(t)$ as $t \to \infty$, $i \in \mathcal{V}^*$;
- the performance constraints imposed on distance errors in (20) are never violated, which further guarantees the collision avoidance (9) and connectivity maintenance (11) among neighboring robots during the formation motion.

IV. FORMATION CONTROL DESIGN

The time derivative of the squared distance error $\eta_{ij}(t)$ along (3)–(6) produces

$$\dot{\eta}_{ij}(t) = 2p_{ij}^T(t)[\dot{p}_i(t) - \dot{p}_j(t)], \ (i,j) \in \mathcal{E}^*$$
 (23)

where $p_{ij}(t)$ is the relative position between the robot i and its neighbor j, $\dot{p}_*(t) = [\cos \theta_*(t)v_*(t) \sin \theta_*(t)v_*(t)]^T$, $* \in \{i, j\}$

with $\theta_*(t)$ and $v_*(t)$ being heading angle and linear velocity input, respectively. Consider the following transformed error in the *universal barrier* function [38] corresponding to each edge in the rigid framework:

$$\sigma_{ij}(t) = \frac{\bar{z}_{ij}\underline{z}_{ij}z_{ij}(t)}{\left(\bar{z}_{ij} - z_{ij}(t)\right)\left(z_{ij}(t) + \underline{z}_{ij}\right)}, \quad (i, j) \in \mathcal{E}^*$$
 (24)

where \underline{z}_{ij} and \bar{z}_{ij} are positive constraints, and $z_{ij}(t)$ in (21) is the error variable.

Remark 1: The transformed error $\sigma_{ij}(t)$ in (24) grows to infinity whenever $z_{ij}(t)$ approaches the boundaries, that is, $\sigma_{ij}(t) \to +\infty$ as $z_{ij}(t) \to \bar{z}_{ij}$ or $\sigma_{ij}(t) \to -\infty$ as $z_{ij}(t) \to -z_{ij}$. Furthermore, $\sigma_{ij}(t) = 0$ if and only if $z_{ij}(t) = 0$. In addition, when there are no constraint requirements on $z_{ij}(t)$, which is equivalent to $\bar{z}_{ij} = z_{ij} \to +\infty$, it follows $\lim_{\bar{z}_{ij} = z_{ij} \to +\infty} \sigma_{ij}(t) = z_{ij}(t)$. Therefore, the proposed barrier function can address both symmetric and asymmetric constraint problems, and can also work for the multiagent systems with no constraints.

The time derivative of (24) along (19), (21), and (23) yields

$$\dot{\sigma}_{ij} = f(z_{ij}) \frac{2p_{ij}^T (\dot{p}_i - \dot{p}_j)}{\beta_{ij}} - g(z_{ij}) \frac{\dot{\beta}_{ij} \sigma_{ij}}{\beta_{ij}}$$
(25)

where

$$f(z_{ij}) = \frac{\bar{z}_{ij}z_{ij}(\bar{z}_{ij}z_{ij} + z_{ij}^2)}{(\bar{z}_{ij} - z_{ij})^2(z_{ij} + z_{ij}^2)^2}, \ g(z_{ij}) = \frac{\bar{z}_{ij}z_{ij} + z_{ij}^2}{(\bar{z}_{ij} - z_{ij})(z_{ij} + z_{ij}^2)}.$$

Then, the control law for formation acquisition and velocity tracking is designed as

$$u_{i}(t) = \begin{bmatrix} u_{ix}(t) \\ u_{iy}(t) \end{bmatrix} = -\sum_{i \in \mathcal{N}} k_{ij} p_{ij}(t) \frac{f(z_{ij})}{\beta_{ij}(t)} \sigma_{ij}^{3}(t) + v_{0}(t) \quad (26)$$

with

$$\theta_{id}(t) = \begin{cases} \operatorname{atan2}(u_{iy}(t), u_{ix}(t)), & \text{if } u_i(t) \neq 0 \\ 0, & \text{if } u_i(t) = 0 \end{cases}$$

where $k_{ij} > 0$ is the control gain, $v_0(t)$ is the desired swarm velocity with its upper bound being $||\bar{v}_0||$, and $atan2(u_{iy}(t), u_{ix}(t))$ is the arctangent function with two arguments returning the appropriate quadrant of the angle of point $(u_{iy}(t), u_{ix}(t))$ as a numeric value in the range $(-\pi, \pi]$. Then, the angle error between heading angle of the robot i and the direction of u_i is defined as

$$\tilde{\theta}_i(t) = \theta_i(t) - \theta_{id}(t) \tag{27}$$

which is further restricted by the performance constraint to ensure $|\tilde{\theta}_i(t)| < \tilde{\theta}_{i,\text{max}}$, for $t \ge 0$, that is

$$-\tilde{\theta}_{i,\max}\beta_{\tilde{\theta}_i}(t) < \tilde{\theta}_i(t) < \tilde{\theta}_{i,\max}\beta_{\tilde{\theta}_i}(t)$$
 (28)

where $\beta_{\tilde{\theta}_i}(t)$ is the performance function with $\beta_{\tilde{\theta}_i}(0) = 1$ defined in (19) and, thus, $\tilde{\theta}_{i,\text{max}} > 0$ is the upper bound of $|\tilde{\theta}_i(t)|$. Consider the following error variable:

$$z_{\tilde{\theta_i}}(t) = \frac{\tilde{\theta_i}(t)}{\beta_{\tilde{\theta_i}}(t)}$$
 (29)

which satisfies $-\tilde{\theta}_{i,\text{max}} < z_{\tilde{\theta}_i}(t) < \tilde{\theta}_{i,\text{max}}$ in view of (28) According to (24), the error transformation is given by

$$\sigma_{\tilde{\theta}_i}(t) = \frac{\tilde{\theta}_{i,\max}^2 z_{\tilde{\theta}_i}(t)}{\tilde{\theta}_{i,\max}^2 - z_{\tilde{\theta}_i}^2(t)}.$$
 (30)

The control laws are designed as

$$v_i = \frac{1}{\cos \tilde{\theta}_i} ||u_i|| \tag{31}$$

$$w_{i} = -k_{1wi}\tilde{\theta}_{i,\max}^{2}\beta_{\tilde{\theta}_{i}}\sigma_{\tilde{\theta}_{i}} + \frac{\tilde{\theta}_{i}\dot{\beta}_{\tilde{\theta}_{i}}}{\beta_{\tilde{\theta}_{i}}} + \dot{\theta}_{id}$$
$$-k_{2wi}\beta_{\tilde{\theta}_{i}} \left(\frac{\tilde{\theta}_{i,\max}^{2} - z_{\tilde{\theta}_{i}}^{2}}{\tilde{\theta}_{i,\max}^{2}}\right)^{2} |\sigma_{\tilde{\theta}_{i}}|^{\frac{1}{2}} \operatorname{sign}\left(\sigma_{\tilde{\theta}_{i}}\right) \quad (32)$$

where $k_{1wi} > 0$ and $k_{2wi} > 0$ are control gains. The singularity problem arises in the controller (31) when $\cos \tilde{\theta}_i \rightarrow 0$. To avoid such a problem, the controller (32) is required to guarantee that the constraint (28) is *never* violated, which further fulfills the condition that $|\tilde{\theta}_i(t)| < \tilde{\theta}_{i,\max} \le \pi/2$. Taking the time derivative of $\theta_{id}(t)$ gives

$$\dot{\theta}_{id} = \begin{cases} \frac{u_i^T H \dot{u}_i}{||u_i||^2}, & \text{if } u_i \neq 0\\ 0, & \text{if } u_i = 0 \end{cases}$$

where

$$\dot{u}_i = -\sum_{i \in \mathcal{N}_i} k_{ij} \left(p_{ij} \frac{f(z_{ij})}{\beta_{ij}} \sigma_{ij}^3 \right)' + \dot{v}_0, \ H = \begin{bmatrix} 0 & 1 \\ -1 & 0 \end{bmatrix}.$$

Note that the time derivatives of p_{ij} , $[f(z_{ij})/\beta_{ij}]$, and σ_{ij} in \dot{u}_i are computable, which are given as follows. It follows from (3), (5), (27), and (31) that $\dot{p}_{ij} = \dot{p}_i - \dot{p}_j$ given by:

$$\dot{p}_* = Q(\tilde{\theta}_*)u_*, \ * \in \{i, j\}$$
(33)

where

$$Q(\tilde{\theta}_*) = \begin{bmatrix} 1 & -\tan\tilde{\theta}_* \\ \tan\tilde{\theta}_* & 1 \end{bmatrix}.$$

Moreover, $\dot{\sigma}_{ij}$ is given in (25) and the time derivative of $[f(z_{ij})/\beta_{ij}]$ can be calculated as

$$\frac{\mathrm{d}\left(\frac{f(z_{ij})}{\beta_{ij}}\right)}{\mathrm{d}t} = \frac{\zeta\left(z_{ij}\right)\left[2p_{ij}^{T}(\dot{p}_{i}-\dot{p}_{j})-\dot{\beta}_{ij}z_{ij}\right]-\dot{\beta}_{ij}f\left(z_{ij}\right)}{\beta_{ij}^{2}}$$

where

$$\zeta(z_{ij}) = \frac{2\bar{z}_{ij}z_{ij}^3 + 6(\bar{z}_{ij}z_{ij})^2 z_{ij} - 2\bar{z}_{ij}^3 z_{ij}^2 + 2\bar{z}_{ij}^2 z_{ij}^3}{(\bar{z}_{ii} - z_{ij})^3 (z_{ij} + z_{ii})^3}.$$

The Lyapunov function candidate is defined as

$$V\left(\sigma_{\tilde{\theta}_i}\right) = \frac{1}{2}\sigma_{\tilde{\theta}_i}^2 \tag{34}$$

whose time derivative along (27)-(32) produces

$$\dot{V}\left(\sigma_{\tilde{\theta}_{i}}\right) \leq -k_{1wi}\sigma_{\tilde{\theta}_{i}}^{4} - k_{2wi}|\sigma_{\tilde{\theta}_{i}}|^{\frac{3}{2}} \tag{35}$$

which implies

$$\dot{V}\left(\sigma_{\tilde{\theta}_i}\right) \leq -\alpha_i V\left(\sigma_{\tilde{\theta}_i}\right)^2 - \rho_i V\left(\sigma_{\tilde{\theta}_i}\right)^{\frac{3}{4}}.$$

Using Lemmas 4 and 5, the angle error $\tilde{\theta}_i$ converges to zero in fixed time with $\alpha_i = 4k_{1wi}$, $\rho_i = 2^{(3/4)}k_{2wi}$, and the settling time can be estimated by $T(\tilde{\theta}_i) \leq T(\tilde{\theta}_i)_{\max} := (1/\alpha_i) + (4/\rho_i)$. Therefore, for the entire multiagent system, all angle errors converge to zero within a fixed-time bounded by $T(\tilde{\theta}) = \max\{T(\tilde{\theta}_i)\}, i \in \mathcal{V}^*$. Next, we will show that the constraint on $\tilde{\theta}_i(t)$ is never violated for $t \geq 0$. Completing the squares, for any variable $x \in \mathbb{R}$, we obtain

$$(x^2 - 1)^2 \ge 0 \Rightarrow -2x^2 + 1 \ge -x^4. \tag{36}$$

Substituting (36) into (35) yields $\dot{V}(\sigma_{\tilde{\theta}_i}) \leq -4k_{1wi}^{(1/2)}V(\sigma_{\tilde{\theta}_i}) + 1$, which implies

$$V\left(\sigma_{\tilde{\theta}_{i}}\right) \leq \left(V\left(\sigma_{\tilde{\theta}_{i,0}}\right) - \frac{1}{4}k_{1wi}^{-\frac{1}{2}}\right) \exp\left(-4k_{1wi}^{\frac{1}{2}}t\right) + \frac{1}{4}k_{1wi}^{-\frac{1}{2}}.$$

It is clear that $V(\sigma_{\tilde{\theta}_i})$ is bounded by initial condition $V(\sigma_{\tilde{\theta}_{i,0}})$, that is, $V(\sigma_{\tilde{\theta}_{i,0}}) \le \iota_i$ for $t \ge 0$. It follows from (34) that:

$$|\sigma_{\tilde{\theta}_i}| \le \sqrt{2\iota_i}.\tag{37}$$

In view of (30), the boundedness of $\sigma_{\tilde{\theta}_i}(t)$ implies the satisfaction of constraint on $z_{\tilde{\theta}_i}(t)$, that is, $-\tilde{\theta}_{i,\max} < z_{\tilde{\theta}_i}(t) < \tilde{\theta}_{i,\max}$ holds. According to (28) and (29), the angle error $\tilde{\theta}_i(t)$ always evolves within the boundary, that is, $|\tilde{\theta}_i(t)| < \tilde{\theta}_{i,\max}\beta_{\tilde{\theta}_i}(t)$, which has the maximal value $\tilde{\theta}_{i,\max}$ at t=0. Therefore, the singularity problem in the controller (31) is avoided with $\tilde{\theta}_{i,\max} \leq \pi/2$.

Next, constructing the following Lyapunov function candidate:

$$V(\sigma) = \frac{1}{4} \sum_{(i,j) \in \mathcal{E}^*} k_{ij} \sigma_{ij}^4 = \frac{1}{4} \left(\sigma^3\right)^T K \sigma \tag{38}$$

where $\sigma \in \mathbb{R}^l$ and $\sigma^3 \in \mathbb{R}^l$, respectively, are the stacked vectors of σ_{ij} and σ^3_{ij} with $\sigma^3 = [\dots, \sigma^3_{ij}, \dots,]^T$, $(i, j) \in \mathcal{E}^*$, and $K = \operatorname{diag}(k_{ij}) \in \mathbb{R}^{l \times l}$. $\dot{\sigma}_{ij}$ in (25) can be rewritten in matrix form as

$$\dot{\sigma} = 2\Xi R \dot{p} - \Theta \sigma \tag{39}$$

where $R \in \mathbb{R}^{l \times 2n}$ is a shorthand notation for R(p) representing the rigidity matrix, $\dot{p} = [\dot{p}_1^T, \dots, \dot{p}_n^T]^T \in \mathbb{R}^{2n}, \ \Xi = \operatorname{diag}(f(z_{ij})/\beta_{ij}) \in \mathbb{R}^{l \times l}$, and $\Theta = \operatorname{diag}(g(z_{ij})\dot{\beta}_{ij}/\beta_{ij}) \in \mathbb{R}^{l \times l}$, for $(i,j) \in \mathcal{E}^*$ and the same ordering as in (1). According to (33), \dot{p} can be rewritten as

$$\dot{p} = \mathbf{Q}u \tag{40}$$

where $\mathbf{Q} = \operatorname{diag}(Q(\tilde{\theta_i})) \in \mathbb{R}^{2n \times 2n}$ and $u \in \mathbb{R}^{2n}$ is the stacked vector of u_i , $i \in \mathcal{V}^*$. Substituting (26) into (40), we obtain

$$\dot{p} = \mathbf{Q}\Big(-R^T \Xi K \sigma^3 + 1_n \otimes \nu_0\Big). \tag{41}$$

From (33), $Q(\hat{\theta}_i)$ can be rewritten as

$$Q\Big(\tilde{\theta}_i\Big) = I_2 + \tan \tilde{\theta}_i \begin{bmatrix} 0 & -1 \\ 1 & 0 \end{bmatrix}.$$

Hence, we obtain

$$\mathbf{Q} = \mathbf{I}_{2n} + \mathbf{Q}^* \tag{42}$$

where $\mathbf{Q}^* = \operatorname{diag}\left(\begin{bmatrix} 0 & -\tan \tilde{\theta}_i \\ \tan \tilde{\theta}_i & 0 \end{bmatrix}\right) \in \mathbb{R}^{2n \times 2n}$. Note that \mathbf{Q}^* is a skew symmetric matrix, which has the property that $X^T\mathbf{Q}^*X = 0$ for non zero vector X. Therefore, differentiating (38) along (39)–(42) gives

$$\dot{V}(\sigma) = -2\left(\sigma^{3}\right)^{T} K \Xi R R^{T} \Xi K \sigma^{3} + 2\left(\sigma^{3}\right)^{T} K \Xi R (1_{n} \otimes v_{0})$$

$$-2\left(\sigma^{3}\right)^{T} K \Xi R \mathbf{Q}^{*} R^{T} \Xi K \sigma^{3} - \left(\sigma^{3}\right)^{T} K \Theta \sigma$$

$$+2\left(\sigma^{3}\right)^{T} K \Xi R \mathbf{Q}^{*} (1_{n} \otimes v_{0}). \tag{43}$$

Using the property of skew symmetric matrix and Lemma 1, $\dot{V}(\sigma)$ in (43) leads to

$$\dot{V}(\sigma) = -2\left(\sigma^{3}\right)^{T} K \Xi R R^{T} \Xi K \sigma^{3} - \left(\sigma^{3}\right)^{T} K \Theta \sigma$$

$$+ 2\left(\sigma^{3}\right)^{T} K \Xi R \mathbf{Q}^{*} (1_{n} \otimes v_{0}). \tag{44}$$

Furthermore, by Young's inequality, we have

$$2(\sigma^{3})^{T} K \Xi R \mathbf{Q}^{*}(1_{n} \otimes \nu_{0}) \leq (\sigma^{3})^{T} K \Xi R R^{T} \Xi K \sigma^{3} + (1_{n} \otimes \nu_{0})^{T} \mathbf{Q}^{*T} \mathbf{Q}^{*}(1_{n} \otimes \nu_{0})$$

where in view of (42), $\mathbf{Q}^{*T}\mathbf{Q}^* \in \mathbb{R}^{2n \times 2n}$ is given as

$$\mathbf{Q}^{*T}\mathbf{Q}^* = \operatorname{diag}\left(\begin{bmatrix} \tan^2 \tilde{\theta}_i & 0\\ 0 & \tan^2 \tilde{\theta}_i \end{bmatrix}\right).$$

Therefore, the term $2(\sigma^3)^T K \Xi R \mathbf{Q}^* (1_n \otimes v_0)$ in (44) leads to

$$2(\sigma^{3})^{T} K \Xi R \mathbf{Q}^{*}(1_{n} \otimes \nu_{0}) \leq (\sigma^{3})^{T} K \Xi R R^{T} \Xi K \sigma^{3} + n \max(\tan^{2} \tilde{\theta}_{i}) ||\bar{\nu}_{0}||^{2}$$
(45)

where $||\bar{v}_0||$ is the upper bound of v_0 . The boundedness of $\sigma_{\tilde{\theta}_i}(t)$ in (37) indicates that $|\tilde{\theta}_i(t)| < \tilde{\theta}_{i,\max}\beta_{\tilde{\theta}_i}(t) \le \pi/2$. Thus, $\tan^2 \tilde{\theta}_i$ is bounded, that is, $\tan^2 \tilde{\theta}_i < c_{\tilde{\theta}_i}$ with $c_{\tilde{\theta}_i}$ being positive constant. Moreover, using Lemma 3, it follows $\lambda_{\min}(RR^T) \ge c_r$ with a constant $c_r > 0$. Hence, substituting (45) into (44) produces

$$\dot{V}(\sigma) \le -c_r \left(\sigma^3\right)^T K \Xi \Xi K \sigma^3 - \left(\sigma^3\right)^T K \Theta \sigma + n \max \left(c_{\tilde{\varrho}_i}\right) ||\bar{v}_0||^2.$$
(46)

Theorem 1: Under Assumption 1, consider the desired rigidity formation $\mathcal{F}^* = (\mathcal{G}^*, p^*)$, robot kinematics (3), and control laws (31) and (32). If control gains k_{1wi} , k_{2wi} $i \in \mathcal{V}^*$, and k_{ij} , $(i,j) \in \mathcal{E}^*$ are chosen such that $k_{1wi} > 0$, $k_{2wi} > 0$, and $k_{ij} > 0$, then we have the following results.

- The performance constraints imposed on distance errors in (20) are never violated, which further guarantees the collision avoidance (9) and connectivity maintenance (11) among neighboring robots during the formation motion.
- 2) The distance errors $e_{ij}(t)$, $(i,j) \in \mathcal{E}^*$ converge to a small neighborhood of zero in a fixed settling time.
- 3) $\mathcal{F}(t) \to \operatorname{Iso}(\mathcal{F}^*)$ as $t \to \infty$ which is equivalent to $e_{ij}(t) \to 0$ as $t \to \infty$, $(i,j) \in \mathcal{E}^*$.
- 4) All robots move with the desired swarm velocity $v_0(t) \in \mathbb{R}^2$, that is, $\dot{p}_i(t) \to v_0(t)$ as $t \to \infty$, $i \in \mathcal{V}^*$.

Proof 1): There exists a scalar $\varpi \in (0, 1)$ such that $\dot{V}(\sigma)$ in (46) can be rewritten as

$$\dot{V}(\sigma) \le -(1 - \varpi)c_r \left(\sigma^3\right)^T K \Xi \Xi K \sigma^3 - \left(\sigma^3\right)^T K \Theta \sigma$$
$$- \varpi c_r \left(\sigma^3\right)^T K \Xi \Xi K \sigma^3 + n \max \left(c_{\tilde{\theta}_i}\right) ||\bar{v}_0||^2. \tag{47}$$

It can be concluded that $\dot{V}(\sigma) \leq 0$ as long as

$$-\varpi c_r \left(\sigma^3\right)^T K \Xi \Xi K \sigma^3 - \left(\sigma^3\right)^T K \Theta \sigma \le 0 \tag{48}$$

and

$$-(1-\varpi)c_r(\sigma^3)^T K\Xi\Xi K\sigma^3 + n\max(c_{\tilde{\theta_i}})||\bar{v}_0||^2 \le 0.(49)$$

First, we discuss a sufficient condition for (48). Substituting K, Ξ , and Θ defined in (39) into (48) yields

$$-\varpi c_r k_{ij} f(z_{ij})^2 \sigma_{ij}^2 - g(z_{ij}) \beta_{ij} \dot{\beta}_{ij} \leq 0.$$

In view of β_{ij} defined in (19), $f(z_{ij})$ and $g(z_{ij})$ defined in (25) where $(\bar{z}_{ij} - z_{ij})^4 (z_{ij} + \underline{z}_{ij})^4 \ge 0$ and $\bar{z}_{ij}\underline{z}_{ij} + z_{ij}^2 \ge \bar{z}_{ij}\underline{z}_{ij} > 0$, we obtain

$$\frac{\gamma_{ij}(\beta_{ij,0}-\beta_{ij,\infty})e^{-\gamma_{ij}t}\beta_{ij}(\bar{z}_{ij}-z_{ij})^3(z_{ij}+\underline{z}_{ij})^3}{\left(\bar{z}_{ij}\underline{z}_{ij}\right)^3}\leq \varpi c_r k_{ij}\sigma_{ij}^2.$$

Note that $(\bar{z}_{ij} - z_{ij})(z_{ij} + \underline{z}_{ij})$ has the maximal value $(\bar{z}_{ij} + \underline{z}_{ij})^2/4 > 0$, and $e^{-\gamma_{ij}t}$ has the maximal value of 1. Hence, we obtain the following sufficient condition for (48):

$$\lambda_1 \leq |\sigma_{ij}|, \ \lambda_1 = \sqrt{\frac{\gamma_{ij} (\beta_{ij,0} - \beta_{ij,\infty}) \beta_{ij,0} (\bar{z}_{ij} + \underline{z}_{ij})^6}{64 (\bar{z}_{ij}\underline{z}_{ij})^3 \varpi c_r k_{ij}}}.$$

Second, we discuss a sufficient condition for (49). Substituting K, Ξ , and Θ defined in (39) into (49), along with $f(z_{ij})$ from (25) yields

$$n \max \left(c_{\tilde{\theta}_i} \right) ||\bar{v}_0||^2 \leq \frac{(1 - \varpi) c_r k_{ij}^2 \left(\bar{z}_{ij} \underline{z}_{ij} \right)^2 z_{ij}^4}{\beta_{ij}^2 \left(\bar{z}_{ij} - z_{ij} \right)^4 \left(z_{ij} + \underline{z}_{ij} \right)^4} \sigma_{ij}^6.$$

Thus, we obtain the following sufficient condition for (49):

$$\lambda_2 \leq |\sigma_{ij}|, \ \lambda_2 = \sqrt[10]{\frac{n \max\left(c_{\tilde{\theta}_i}\right) ||\bar{v}_0||^2 \left(\bar{z}_{ij}\underline{z}_{ij}\right)^2 \beta_{ij,0}^2}{(1-\varpi)c_r k_{ij}^2}}.$$

As a result, $V(\sigma)$ is nonincreasing as long as $|\sigma_{ij}| \ge \max\{\lambda_1, \lambda_2\}$. Thus, it follows from (38) that σ_{ij} is bounded, which indicates the constraint requirement on z_{ij} is never violated according to (22). Then, the constraint (18) is satisfied, which indicates the satisfaction of (17) and (20). Therefore, the inequality (14) holds, which implies that collision avoidance (9) and connectivity maintenance (11) among neighboring robots are guaranteed during the formation motion.

Proof 2): The boundedness of σ_{ij} in proof 1) indicates that $f(z_{ij})$ and $g(z_{ij})$ defined in (25) are also bounded since the constraint requirement $-\underline{z}_{ij} < z_{ij}(t) < \bar{z}_{ij}$ is satisfied. Thus, we have $\underline{c}_{f_{ij}} < f(z_{ij}) < \bar{c}_{f_{ij}}$ and $\underline{c}_{g_{ij}} < g(z_{ij}) < \bar{c}_{g_{ij}}$ with $\underline{c}_{f_{ij}}$,

 $\bar{c}_{f_{ij}}$, $\underline{c}_{g_{ij}}$, and $\bar{c}_{g_{ij}}$ being positive constants. By completion of squares, we obtain

$$\frac{g(z_{ij})\dot{\beta}_{ij}}{\beta_{ii}}k_{ij}\sigma_{ij}^4 \le c_r\epsilon k_{ij}^2\sigma_{ij}^8 + \frac{1}{4c_r\epsilon} \left(\frac{g(z_{ij})\dot{\beta}_{ij}}{\beta_{ii}}\right)^2$$

where $\epsilon > 0$ is an arbitrary small constant, which implies that the term $(\sigma^3)^T K\Theta \sigma$ in (46) is bounded by

$$\left(\sigma^{3}\right)^{T} K \Theta \sigma = \sum_{(i,j) \in \mathcal{E}^{*}} \left(k_{ij} \frac{g(z_{ij}) \dot{\beta}_{ij}}{\beta_{ij}} \sigma_{ij}^{4}\right)$$

$$\leq \sum_{(i,j) \in \mathcal{E}^{*}} \left(c_{r} \epsilon k_{ij}^{2} \sigma_{ij}^{8} + c_{ij}\right) \tag{50}$$

where $c_{ij} = \bar{c}_{g_{ij}}^2 \gamma_{ij}^2 (\beta_{ij,0} - \beta_{ij,\infty})^2 / 4c_r \epsilon \beta_{ij,\infty}^2$. Moreover, in view of (24) and (25), we have $f(z_{ij}) > (1/\bar{z}_{ij}\underline{z}_{ij})\sigma_{ij}^2 \ge 0$, which implies that

$$-\frac{k_{ij}^{2}f(z_{ij})^{2}}{\beta_{ij}^{2}}\sigma_{ij}^{6} \leq -\frac{k_{ij}^{2}f(z_{ij})}{\bar{z}_{ij}z_{ij}\beta_{ij}^{2}}\sigma_{ij}^{8} \leq -\frac{k_{ij}^{2}\underline{c}_{fij}}{\bar{z}_{ij}z_{ij}\beta_{ij,0}^{2}}\sigma_{ij}^{8}.$$
 (51)

There exists a scalar $\kappa \in (0, 1)$ such that $\dot{V}(\sigma)$ in (46) can be rewritten as

$$\dot{V}(\sigma) \le -(1 - \kappa)c_r \left(\sigma^3\right)^T K \Xi \Xi K \sigma^3 - \left(\sigma^3\right)^T K \Theta \sigma$$
$$-\kappa c_r \left(\sigma^3\right)^T K \Xi \Xi K \sigma^3 + n \max\left(c_{\tilde{\theta}_i}\right) ||\bar{v}_0||^2 \tag{52}$$

which yields

$$\dot{V}(\sigma) \leq -(1 - \kappa)c_r \left(\sigma^3\right)^T K \Xi \Xi K \sigma^3 + C^*$$

$$+ \sum_{(i,j) \in \mathcal{E}^*} \left(c_r \epsilon k_{ij}^2 \sigma_{ij}^8 - \kappa c_r \frac{k_{ij}^2 c_{f_{ij}}}{\bar{z}_{ij} z_{ij} \beta_{ij,0}^2} \sigma_{ij}^8\right)$$
(53)

by inequalities (50) and (51), where $C^* = n \max(c_{\tilde{\theta_i}}) ||\bar{v}_0||^2 + \sum_{(i,j) \in \mathcal{E}^*} c_{ij}$. Let the arbitrary small constant ϵ satisfy $\epsilon \leq \min(\kappa c_{f_{ij}}/\bar{z}_{ij}z_{ij}\beta_{ij,0}^2)$, $(i,j) \in \mathcal{E}^*$ such that $\dot{V}(\sigma)$ in (52) leads to

$$\dot{V}(\sigma) \le -(1 - \kappa)c_r(\sigma^3)^T K \Xi \Xi K \sigma^3 + C^*. \tag{54}$$

Next, we will show the fixed-time convergence of distance errors. $\dot{V}(\sigma)$ in (54) can be rewritten as

$$\dot{V}(\sigma) \le -(1 - \kappa)(1 - \varrho)c_r \left(\sigma^3\right)^T K \Xi \Xi K \sigma^3$$

$$-\varrho(1 - \kappa)c_r \left(\sigma^3\right)^T K \Xi \Xi K \sigma^3 + C^* \tag{55}$$

where $\varrho \in (0, 1)$ is a scalar. Completing the squares, for any variable $x \in \mathbb{R}$, we obtain

$$(|x|^3 - 1)^2 \ge 0 \Rightarrow -2|x|^3 + 1 \ge -x^6$$

which implies that the following inequality holds:

$$-\left(\sigma^{3}\right)^{T} K \Xi \Xi K \sigma^{3} \leq -2 \sum_{(i,j) \in \mathcal{E}^{*}} k_{ij} \frac{f(z_{ij})}{\beta_{ij}} |\sigma_{ij}|^{3} + l \quad (56)$$

where $\dim(\mathcal{E}^*) = l$. Substituting (56) into (55) yields

$$\dot{V}(\sigma) \le -\chi_1 \sum_{(i,j) \in \mathcal{E}^*} \sigma_{ij}^6 - \chi_2 \sum_{(i,j) \in \mathcal{E}^*} |\sigma_{ij}|^3 + C$$

where $\chi_1 = (1 - \kappa)(1 - \varrho)c_r\lambda_{\min}(\Xi)^2\lambda_{\min}(K)^2$, $\chi_2 = 2\varrho(1-\kappa)c_r\lambda_{\min}(\Xi)\lambda_{\min}(K)$, with $\lambda_{\min}(\Xi) = \min(f(z_{ij})/\beta_{ij}) \ge \min(c_{f_{ij}}/\beta_{ij},0) > 0$, and $C = C^* + \varrho(1-\kappa)c_rl$ being a positive constant. Using Lemma 5, we have

$$\dot{V}(\sigma) \le -\alpha V(\sigma)^{\frac{3}{2}} - \rho V(\sigma)^{\frac{3}{4}} + C \tag{57}$$

where $\alpha=2^3\chi_1l^{-(1/2)}\lambda_{\max}(K)^{-(3/2)}$ and $\rho=2^{(3/2)}\chi_2\lambda_{\max}(K)^{-(3/4)}$. There exists a scalar $\varepsilon\in(0,1)$ such that $\dot{V}(\sigma)$ in (57) can be rewritten as

$$\dot{V}(\sigma) \le -\alpha(1-\varepsilon)V(\sigma)^{\frac{3}{2}} - \rho V(\sigma)^{\frac{3}{4}} - \alpha\varepsilon V(\sigma)^{\frac{3}{2}} + C$$

which implies that $\dot{V}(\sigma) \leq -\alpha(1-\varepsilon)V(\sigma)^{(3/2)} - \rho V(\sigma)^{(3/4)}$ when $(C/\alpha\varepsilon) \leq V(\sigma)^{(3/2)}$. Thus, according to Lemma 4, $V(\sigma)$ converges into the set $\{V(\sigma)|V(\sigma) < (C/\alpha\varepsilon)^{(2/3)}\}$ in fixed time. Furthermore, in view of (38), we obtain

$$|\sigma_{ij}| < \varsigma \tag{58}$$

where $\zeta = 2^{(1/2)} k_{ij}^{-(1/4)} (C/\alpha \varepsilon)^{(1/6)} > 0$ can be designed as a small neighborhood of the origin by properly selecting k_{ij} . From (24) and (58), we obtain

$$-\underline{\Lambda}_{ij} < z_{ij}(t) < \bar{\Lambda}_{ij} \tag{59}$$

where

$$\underline{\Lambda}_{ij} = \frac{\varsigma(\underline{z}_{ij} - \bar{z}_{ij}) - \bar{z}_{ij}\underline{z}_{ij} + \sqrt{(\varsigma\underline{z}_{ij} - \varsigma\bar{z}_{ij} - \bar{z}_{ij}\underline{z}_{ij})^2 + 4\varsigma^2\bar{z}_{ij}\underline{z}_{ij}}}{2\varsigma}$$

and

$$\bar{\Lambda}_{ij} = \frac{\varsigma(\bar{z}_{ij} - \underline{z}_{ij}) - \bar{z}_{ij}\underline{z}_{ji} + \sqrt{(\bar{z}_{ij}\underline{z}_{ij} + \varsigma\underline{z}_{ij} - \varsigma\bar{z}_{ij})^2 + 4\varsigma^2\bar{z}_{ij}\underline{z}_{ij}}}{2\varsigma}$$

As a result, the squared distance errors η_{ij} converge into the set $\Omega_{\eta_{ij}} = \{\eta_{ij}(t) | -\underline{\Lambda}_{ij}\beta_{ij}(t) < \eta_{ij}(t) < \bar{\Lambda}_{ij}\beta_{ij}(t)\}$ which implies that distance errors e_{ij} also converge to a small neighborhood around zero in fixed time.

Proof 3): It is clear from (35) that all angle errors $\tilde{\theta}_i(t)$ converge to the origin in fixed time $T(\tilde{\theta})$, which implies that $\mathbf{Q}^* \to \mathbf{0}$ for $t > T(\tilde{\theta})$ according to (42). Moreover, proof 2) indicates that $g(z_{ij})$ defined in (25) is bounded due to the boundedness of σ_{ij} . In addition, $\dot{\beta}_{ij}(t)$ ultimately decreases to zero. Thus, Θ defined in (39) also ultimately decreases to zero. It is concluded that according to Lemmas 1 and 3 as $t \to \infty$, $\dot{V}(\sigma)$ in (43) leads to

$$\dot{V}(\sigma) \le -2\lambda_{\min}(RR^T)\lambda_{\min}(\Xi)^2\lambda_{\min}(K)^2(\sigma^3)^T\sigma^3$$

which indicates that the σ_{ij} asymptotically converges to the origin. Hence, it is clear from (24), (21), and (16) that $z_{ij} \to 0$, $\eta_{ij} \to 0$, and $e_{ij}(t) \to 0$ as $t \to \infty$.

Proof 4): Because of the boundedness of e_{ij} obtained from proof 1), it is from (7) that d_{ij} is bounded, which indicates the boundedness of rigidity matrix R(p). Moveover, angle errors $\tilde{\theta}_i(t)$ are fixed-time stable according to the analysis result of $V(\sigma_{\tilde{\theta}_i})$ in (35), which implies $\tilde{\theta}_i(t) \to 0$, $Q(\tilde{\theta}_i) \to I_2$, and $\mathbf{Q} \to I_{2n}$ for $t > T(\tilde{\theta})$. Furthermore, according to proof 3), we know that $\sigma_{ij} \to 0$ and $z_{ij} \to 0$ and, thus, $\Xi \to \mathrm{diag}(1/\beta_{ij,\infty})$ as $t \to \infty$. As a result, in terms of (41), $\dot{p} \to 1_n \otimes v_0$, which is equivalent to $\dot{p}_i \to v_0$ as $t \to \infty$.

Remark 2: It is worth noticing that the constrained control laws (31) and (32) are substantially different from the existing distance-based formation controllers presented in [15] where there is no constraint requirement in control design. For comparison, the distance-based formation control laws [15] are recalled as follows:

$$v_{i} = ||u_{i}|| \cos \tilde{\theta}_{i}$$

$$w_{i} = -k_{wi}\tilde{\theta}_{i} + \dot{\theta}_{id}$$

$$u_{i} = \begin{bmatrix} u_{ix} \\ u_{iy} \end{bmatrix} = -\sum_{i \in \mathcal{N}_{i}} k_{ij}p_{ij}\eta_{ij} + v_{0}.$$
(60)

With the concern of constraint requirements in the rigiditybased formation maneuvering, the constrained control design becomes very challenging due to the following two reasons.

- 1) By incorporating the barrier Lyapunov function with control design and analysis for constrained control systems, the time derivative of transform errors $\dot{\sigma}_{ij}(t)$ in (25) is more complicated compared with the time derivative of squared distance error $\dot{\eta}_{ij}(t)$ in (60) in unconstrained systems.
- 2) When the angle error $\tilde{\theta}_i$ is around $\pm \pi/2$, the linear velocity is approximate zero in (60) in the unconstrained system, and explodes to infinity in (31), which implies a risk of the violation of constraint requirements especially in the transient time, and causes the singularity issue in the controller. Consequently, the angle error $\tilde{\theta}_i$ is further restricted within the feasible region $(-\pi/2, \pi/2)$ to prevent the control singularity problem.

Remark 3: The distance errors e_{ii} can converge to a small neighborhood around zero in fixed time by adjusting control gains k_{ij} . When $k_{ij} \rightarrow \infty$, $(i,j) \in \mathcal{E}^*$, we have $k_{ij} = \lambda_{\min}(K) = \lambda_{\max}(K) \rightarrow \infty$. Thus, the constant α in (57) can be rewritten as $\alpha = 2^3 k_{ii}^{(1/2)} (1 \kappa$)(1 - ϱ) $c_r \lambda_{\min}(\Xi)^2 l^{-(1/2)}$. Then, ς in (58) leads to $\varsigma = [(l^{(1/2)}C)/(\varepsilon(1-\kappa)(1-\varrho)c_r\lambda_{\min}(\Xi)^2)]^{1/6}k_{ii}^{-(1/3)} \to 0$ which indicates that the transformed errors σ_{ii} is bounded by ς that can be designed as a small neighborhood of the origin by designing large control gains k_{ij} . Moreover, the error bounds of variables z_{ij} in (59) are also arbitrarily small as $\zeta \to 0$ since by L' Hopital's rule, we have $\lim_{\zeta \to 0} \underline{\Lambda}_{ii} = 0$ and $\lim_{\zeta \to 0} \overline{\Lambda}_{ij} =$ 0. As a result, $\underline{\Lambda}_{ij}\beta_{ij}(t) \to 0$ and $\bar{\Lambda}_{ij}\beta_{ij}(t) \to 0$, which implies that when the squared distance errors η_{ij} converge into the set $\Omega_{\eta_{ij}} = \{\eta_{ij}(t) | -\underline{\Lambda}_{ij}\beta_{ij}(t) < \eta_{ij}(t) < \Lambda_{ij}\beta_{ij}(t) \}, \text{ the distance}$ errors e_{ij} also converge to a small neighborhood around zero.

V. COMPARATIVE SIMULATION STUDIES

To show the improved formation maneuvering performance of the proposed fixed-time controller, we perform a comparative simulation study between the control laws (31), (32) and the existing distance-based formation controller presented in [15]. Consider five identical nonholonomic mobile robots modeled by system (3). The desired translational velocity is given by $v_0(t) = [1 \cos(t)]^T$ m/s. The desired formation \mathcal{E}^* is designed as a regular pentagon with formation topology shown in Fig. 1, which is made infinitesimally and minimally rigid by introducing seven edges, that is,

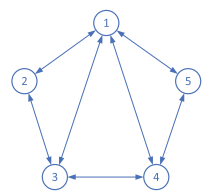


Fig. 1. Formation topology.

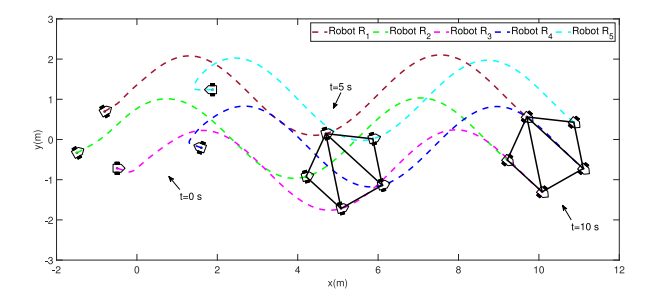


Fig. 2. Phase plane trajectories.

= $\{(1,2), (1,3), (1,4), (1,5), (2,3), (3,4), (4,5)\}$. Let the maximum sensing range $\bar{d}_{ij}=5$ m and the safe distance $\underline{d}_{ij}=0.6$ m, $(i,j)\in\mathcal{E}^*$ with infinitesimally rigid preservation parameter $\mu = 0.12$. To avoid the controller singularity, the upper bound of angle errors is selected as $\theta_{i,\text{max}} = \pi/2$ rad. Without the violation of constraint requirements from collision avoidance and connectivity maintenance, we choose the desired relative distance $d_{\text{des},12} = d_{\text{des},15} =$ $d_{\text{des},23} = d_{\text{des},34} = d_{\text{des},45} = \sqrt{2(1-\cos(2\pi/5))}$ m, and $d_{\text{des},13} = d_{\text{des},14} = \sqrt{2(1 + \cos(\pi/5))}$ m. In accordance with (19), the prescribed performance constraints imposed on the squared distance error and the angle error are formulated as $\beta_{ij} = \beta_{\tilde{\theta}_i} = (1 - 0.05) \exp(-0.6t) + 0.05$. The design parameters in (26) and (32) are taken as $k_{12} = k_{13} = k_{14} = k_{15} =$ $k_{23} = k_{34} = k_{45} = 3$, $k_{1w1} = k_{1w2} = k_{1w3} = k_{1w4} = k_{1w5} = 1$, and $k_{2w1} = k_{2w2} = k_{2w3} = k_{2w4} = k_{2w5} = 1$. The initial positions are $p_1(0) = [-0.8049 \ 0.6951]^T$, $p_2(0) =$ $[-1.4941 - 0.3340]^T$, $p_3(0) = [-0.4940 - 0.7153]^T$, $p_4(0) = [1.6028 - 0.2060]^T$, and $p_5(0) = [1.8808 \ 1.2388]^T$. The initial heading angles are given by $\theta_1(0) = \pi/6$ rad, $\theta_2(0) = \pi/6 \text{ rad}, \ \theta_3(0) = 0 \text{rad}, \ \theta_4(0) = 8\pi/9 \text{rad}, \ \text{and}$ $\theta_5(0) = -\pi \text{ rad}$. In terms of (26) and (27), the initial angle errors are $\tilde{\theta}_1(0) = 0.4234 \text{rad}$, $\tilde{\theta}_2(0) = -0.4539 \text{rad}$, $\tilde{\theta}_3(0) =$ 0.5591rad, $\theta_4(0) = -0.1146$ rad, $\theta_5(0) = -0.2002$ rad, which indicates that all initial angle errors start within the predefined error bounds, that is, $|\tilde{\theta}_i(0)| < \tilde{\theta}_{i,\text{max}} = \pi/2\text{rad}$. The design parameters in the distance-based formation control law (60) presented in [15] are $k_{w1} = k_{w2} = k_{w3} = k_{w4} = k_{w5} = 3$ and $k_{12} = k_{13} = k_{14} = k_{15} = k_{23} = k_{34} = k_{45} = 2$. For comparison, the initial positions and heading angles for the two controllers are the same.

Simulation results are depicted in Figs. 2–10. The phase plane trajectories of nonholonomic robots with different snapshots at 0, 5, and 10 s are illustrated in Fig. 2, where the proposed control laws ensure the convergence to the desired formation of a regular pentagon. Figs. 3–9 show the results of distance errors using the proposed fixed-time controller (31), (32) and the distance-based formation controller [15],

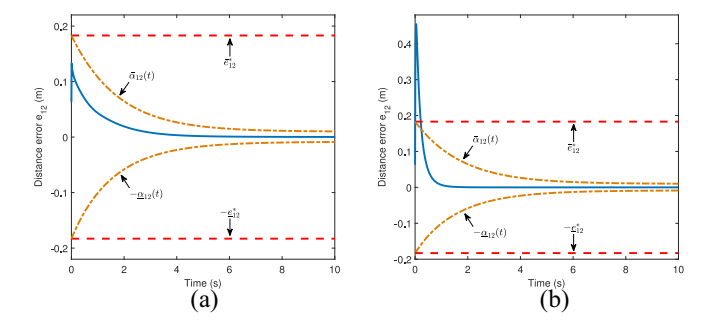


Fig. 3. Profiles of distance error e_{12} . (a) Proposed fixed-time control with prescribed performance. (b) Distance-based formation control [15].

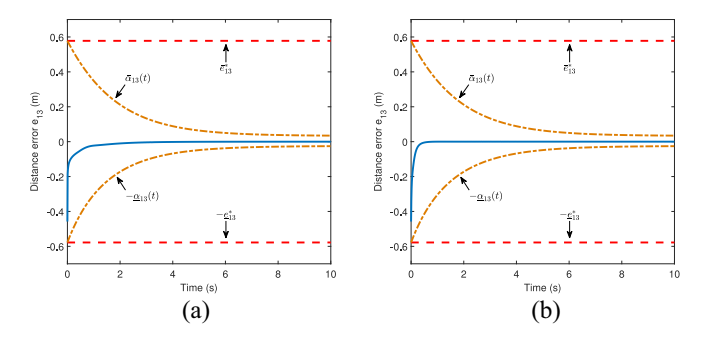


Fig. 4. Profiles of distance error e_{13} . (a) Proposed fixed-time control with prescribed performance. (b) Distance-based formation control [15].

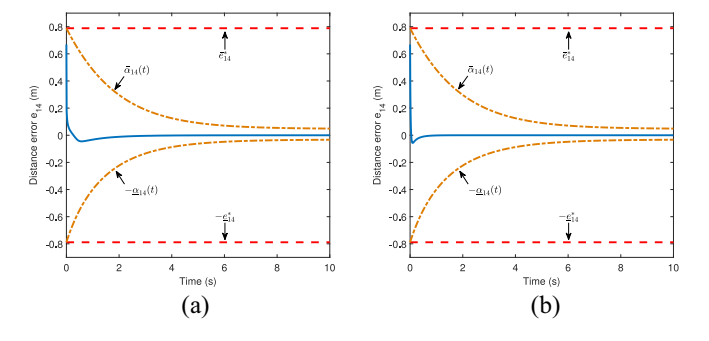


Fig. 5. Profiles of distance error e_{14} . (a) Proposed fixed-time control with prescribed performance. (b) Distance-based formation control [15].

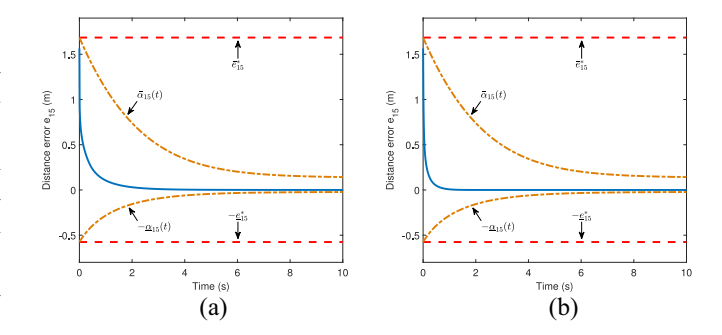


Fig. 6. Profiles of distance error e_{15} . (a) Proposed fixed-time control with prescribed performance. (b) Distance-based formation control [15].

where all distance errors are driven to a small neighborhood of zero. From Figs. 3(a)–9(a), it is clear that the proposed fixed-time formation controller can guarantee that the distance errors always evolve within the prescribed performance bounds $-\underline{\alpha}_{ij}(t)$ and $\bar{\alpha}_{ij}(t)$ given in (20), which further indicates

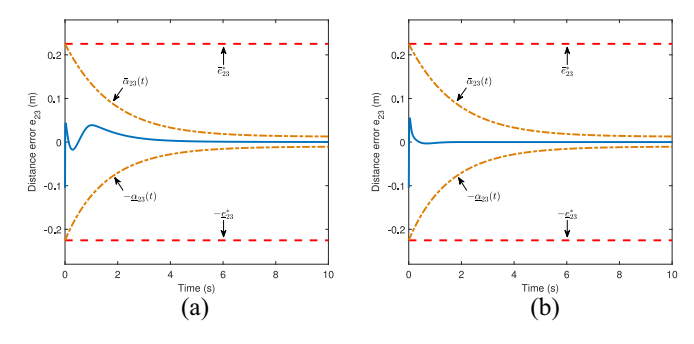


Fig. 7. Profiles of distance error e_{23} . (a) Proposed fixed-time control with prescribed performance. (b) Distance-based formation control [15].

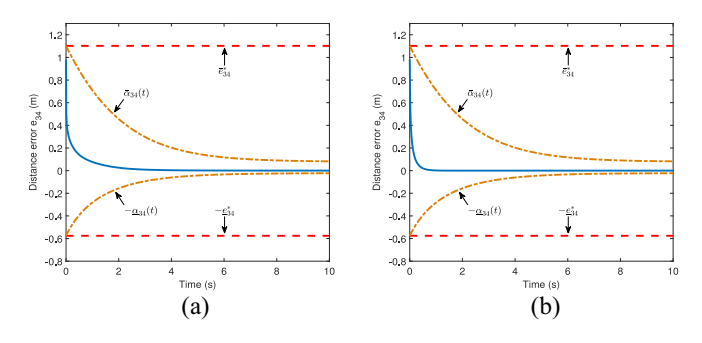


Fig. 8. Profiles of distance error e_{34} . (a) Proposed fixed-time control with prescribed performance. (b) Distance-based formation control [15].

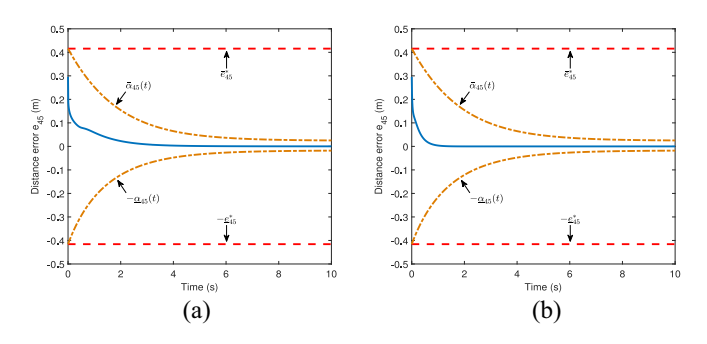


Fig. 9. Profiles of distance error e_{45} . (a) Proposed fixed-time control with prescribed performance. (b) Distance-based formation control [15].

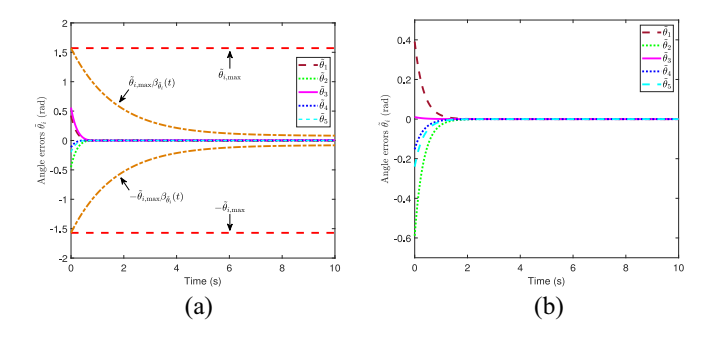


Fig. 10. Profiles of angle errors $\tilde{\theta}_i$. (a) Proposed fixed-time control with prescribed performance. (b) Distance-based formation control [15].

that both connectivity maintenance and collision avoidance $[-\underline{e}_{ij}^*]$ and \bar{e}_{ij}^* given in (14)] are not violated. In comparison, Fig. 3(b) shows the distance error e_{12} has exceeded the allowed maximum bound, which indicates the communication connectivity between neighboring robots is broken. These

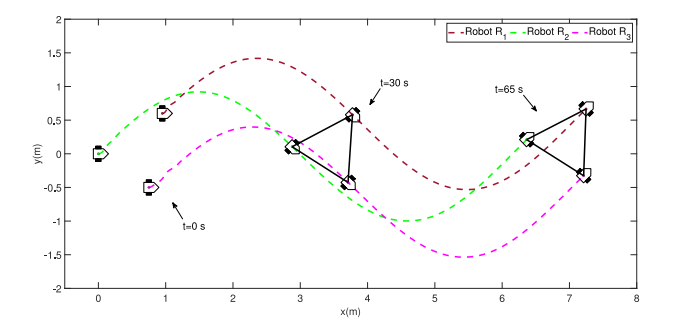


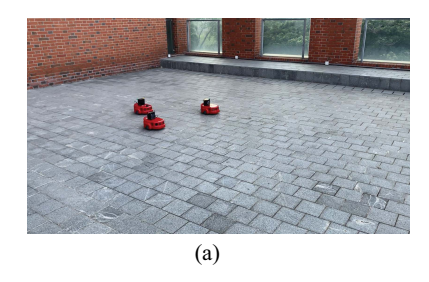
Fig. 11. Phase plane trajectories in the experiment.

results show the advantage of the proposed control protocol with concerns of safety and performance requirements for constrained multiagent systems. In addition, the angle errors are demonstrated in Fig. 10, where the angle errors are enforced to stay within the performance bounds [Fig. 10(a)] and, thus, the singularity problem in the controller (31) is avoided. The angle errors are exponentially stable using the angular control law given in [15], as shown in Fig. 10(b). It should be noted that the initial angle errors are different for the two controllers since θ_{id} resulting from u_i are designed differently [(26) and (60)] even though the initial heading angles of robots are the same.

VI. EXPERIMENT STUDIES

The formation control laws (31) and (32) are experimentally verified on three AmigoBot mobile robots. In the experiment, each AmigoBot accesses to the wireless network via Wi-Fi modules onboard, which enables them to share information and receive control commands. The proposed control laws are executed in a laptop and sent to all robots through Wi-Fi at 10 Hz. The desired translational velocity is given by $v_0(t) = [0.1 \ 0.1 \cos(0.1t)]^T$ m/s. The desired formation \mathcal{E}^* is designed as a regular triangle with three edges \mathcal{E}^* = $\{(1, 2), (1, 3), (2, 3)\}$. Let the maximum sensing range $\bar{d}_{ij} = 5$ m, the safe distance $\underline{d}_{ij} = 0.6$ m, $(i, j) \in \mathcal{E}^*$, and the maximum angle error $\tilde{\theta}_{i,\text{max}} = \pi/2$ rad with infinitesimally rigid preservation parameter $\mu = 0.12$. Without the violation of collision avoidance and connectivity maintenance, we set the desired relative distance $d_{\text{des},12} = d_{\text{des},13} = d_{\text{des},23} = 1\text{m}$. In accordance with (19), the prescribed performance constraints imposed on the squared distance error and the angle error are taken as $\beta_{ij} = (1 - 0.1) \exp(-0.025t) + 0.1$ and $\beta_{\tilde{\theta}_i} =$ $(1-0.1) \exp(-0.03t) + 0.1$, respectively. The design parameters in (26) and (32) are selected as $k_{12} = k_{13} = k_{23} = 1$, $k_{1w1} = k_{1w2} = k_{1w3} = 1$, and $k_{2w1} = k_{2w2} = k_{2w3} = 0.1$. The initial positions are $p_1(0) = [0.95 \ 0.6]^T$, $p_2(0) = [0 \ 0]^T$, and $p_3(0) = [0.75 - 0.5]^T$. The initial heading angles are given by $\theta_1(0) = \theta_2(0) = \theta_3(0) = 0$ rad. In accordance with (26) and (27), the initial angle errors are $\tilde{\theta}_1(0) = -0.3991$ rad, $\tilde{\theta}_2(0) = -0.8971$ rad, and $\tilde{\theta}_3(0) = -0.7498$ rad, which implies that all initial angle errors start within the predefined error bounds, that is, $|\tilde{\theta}_i(0)| < \tilde{\theta}_{i,\text{max}} = \pi/2 \text{ rad.}$

The experimental results are demonstrated in Figs. 11–16. The phase plane trajectories of nonholonomic robots and



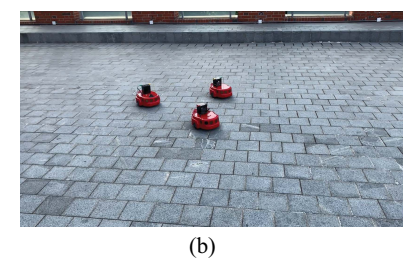




Fig. 12. Snapshots taken in the experiment. (a) t = 0 s. (b) t = 30 s. (c) t = 65 s.

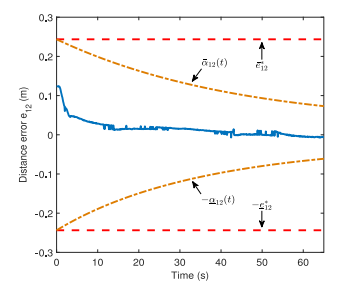


Fig. 13. Profiles of distance error e_{12} .

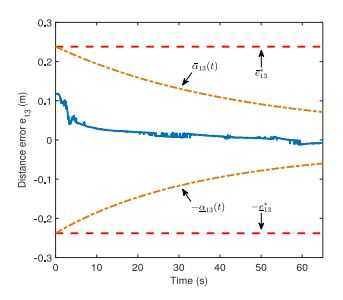


Fig. 14. Profiles of distance error e_{13} .

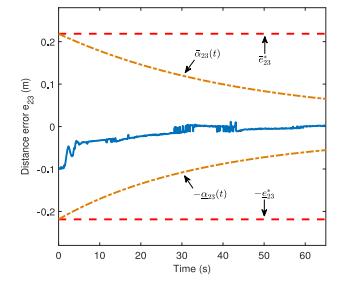


Fig. 15. Profiles of distance error e_{23} .

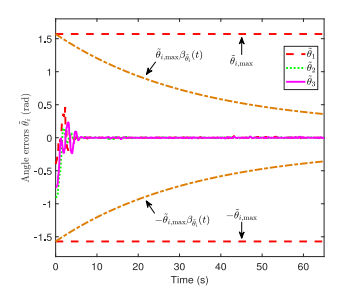


Fig. 16. Profiles of angle errors $\tilde{\theta}_i$.

different snapshots at 0, 30, and 65 s are, respectively, illustrated in Figs. 11 and 12, in which the desired formation of a regular triangle is successfully acquired from the initial

configuration and maintained during the formation motion. Figs. 13–16 show that all of the distance errors (Figs. 13–15) and the angle errors (Fig. 16) stay within their prescribed performance bounds, and converge to a small neighborhood of zero. Accordingly, collision avoidance and connectivity maintenance among neighboring robots are guaranteed, and the controller singularity is avoided.

VII. CONCLUSION

This article has presented a fixed-time rigidity-based formation maneuvering control protocol for nonholonomic multirobot systems with prescribed performance. All robots can track the desired time-varying velocity while converging to the desired shape defined by a minimally and infinitesimally rigid graph. The performance constraints imposed on the distance and angle errors, which can specify their transient and steady-state performances, guarantee collision avoidance and connectivity maintenance among neighboring robots, and avoid the controller singularity issue. Using rigid graph theory, fixed-time control design, universal barrier functions, and Lyapunov synthesis, formation maneuvering control laws are proposed such that the angle errors are fixed-time stable, and the distance errors can converge to a small neighborhood around zero in fixed time and then asymptotically converge to the origin. Future studies will focus on the time-varying maneuvering formation which is scalable and reconfigurable. Another challenging topic is to consider the obstacle avoidance in an obstacle-cluttered environment.

REFERENCES

- H. Duan and D. Zhang, "A binary tree based coordination scheme for target enclosing with micro aerial vehicles," *IEEE/ASME Trans. Mechatronics*, vol. 26, no. 1, pp. 458–468, Feb. 2021.
- [2] S. Zhao and D. Zelazo, "Bearing rigidity and almost global bearing-only formation stabilization," *IEEE Trans. Autom. Control*, vol. 61, no. 5, pp. 1255–1268, May 2016.
- [3] S.-L. Dai, K. Lu, and X. Jin, "Fixed-time formation control of unicycletype mobile robots with visibility and performance constraints," *IEEE Trans. Ind. Electron.*, vol. 68, no. 12, pp. 12615–12625, Dec. 2021.
- [4] H. G. de Marina, B. Jayawardhana, and M. Cao, "Distributed rotational and translational maneuvering of rigid formations and their applications," *IEEE Trans. Robot.*, vol. 32, no. 3, pp. 684–697, Jun. 2016.
- [5] X. Fang, X. Li, and L. Xie, "Distributed formation maneuver control of multiagent systems over directed graphs," *IEEE Trans. Cybern.*, vol. 52, no. 8, pp. 8201–8212, Aug. 2022.
- [6] F. Mehdifar, F. Hashemzadeh, M. Baradarannia, and M. de Queiroz, "Finite-time rigidity-based formation maneuvering of Multiagent systems using distributed finite-time velocity estimators," *IEEE Trans. Cybern.*, vol. 49, no. 12, pp. 4473–4484, Dec. 2019.
- [7] S. Ramazani, R. Selmic, and M. de Queiroz, "Rigidity-based multiagent layered formation control," *IEEE Trans. Cybern.*, vol. 47, no. 8, pp. 1902–1913, Aug. 2017.

- [8] S. Zhao and D. Zelazo, "Localizability and distributed protocols for bearing-based network localization in arbitrary dimensions," *Automatica*, vol. 69, pp. 334–341, Jul. 2016.
- [9] X. Li, C. Wen, X. Fang, and J. Wang, "Adaptive bearing-only formation tracking control for nonholonomic multiagent systems," *IEEE Trans. Cybern.*, vol. 52, no. 8, pp. 7552–7562, Aug. 2022.
- [10] H. Su, C. Chen, Z. Yang, S. Zhu, and X. Guan, "Bearing-based formation tracking control with time-varying velocity estimation," *IEEE Trans. Cybern.*, early access, May 30 2022, doi: 10.1109/TCYB.2022.3169891.
- [11] K. Shojaei, "Neural network formation control of a team of tractore-trailer systems," *Robotica*, vol. 36, no. 1, pp. 39–56, 2018.
- [12] M. Rosenfelder, H. Ebel, and P. Eberhard, "Cooperative distributed nonlinear model predictive control of a formation of differentially-driven mobile robots," *Robot. Auton. Syst.*, vol. 150, Apr. 2022, Art. no. 103993.
- [13] K. Shojaei, "Output-feedback formation control of wheeled mobile robots with actuators saturation compensation," *Nonlinear Dyn.*, vol. 89, pp. 2867–2878, Jul. 2017.
- [14] R. Hou, L. Cui, X. Bu, and J. Yang, "Distributed formation control for multiple non-holonomic wheeled mobile robots with velocity constraint by using improved data-driven iterative learning," *Appl. Math. Comput.*, vol. 395, Apr. 2021, Art. no. 125829.
- [15] M. Khaledyan, T. Liu, V. Fernandez-Kim, and M. de Queiroz, "Flocking and target interception control for formations of nonholonomic kinematic agents," *IEEE Trans. Control Syst. Technol.*, vol. 28, no. 4, pp. 1603–1610, Jul. 2020.
- [16] S.-L. Dai, K. Lu, and J. Fu, "Adaptive finite-time tracking control of Nonholonomic Multirobot formation systems with limited field-ofview sensors," *IEEE Trans. Cybern.*, vol. 52, no. 10, pp. 10695–10708, Oct. 2022.
- [17] Z. Peng, D. Wang, T. Li, and M. Han, "Output-feedback cooperative formation maneuvering of autonomous surface vehicles with connectivity preservation and collision avoidance," *IEEE Trans. Cybern.*, vol. 50, no. 6, pp. 2527–2535, Jun. 2020.
- [18] Y. Liu, P. Shi, and C.-C. Lim, "Collision-free formation control for multi-agent systems with dynamic mapping," *IEEE Trans. Circuits Syst. II, Exp. Briefs*, vol. 67, no. 10, pp. 1984–1988, Oct. 2020.
- [19] Y. Liu, P. Shi, H. Yu, and C.-C. Lim, "Event-triggered probability-driven adaptive formation control for multiple elliptical agents," *IEEE Trans.* Syst., Man, Cybern., Syst., vol. 52, no. 1, pp. 645–654, Jan. 2022.
- [20] H. Duan, Q. Luo, Y. Shi, and G. Ma, "Hybrid particle swarm optimization and genetic algorithm for multi-UAV formation reconfiguration," *IEEE Comput. Intell. Mag.*, vol. 8, no. 3, pp. 16–27, Aug. 2013.
- [21] D. Panagou and V. Kumar, "Cooperative visibility maintenance for leader-follower formations in obstacle environments," *IEEE Trans. Robot.*, vol. 30, no. 4, pp. 831–844, Aug. 2014.
- [22] D. Sakai, H. Fukushima, and F. Matsuno, "Leader-follower navigation in obstacle environments while preserving connectivity without data transmission," *IEEE Trans. Control Syst. Technol.*, vol. 26, no. 4, pp. 1233–1248, Jun. 2018.
- [23] S.-L. Dai, S. He, Y. Ma, and C. Yuan, "Distributed cooperative learning control of uncertain multiagent systems with prescribed performance and preserved connectivity," *IEEE Trans. Neural Netw. Learn. Syst.*, vol. 32, no. 7, pp. 3217–3229, Jun. 2021.
- [24] A. Mondal, C. Bhowmick, L. Behera, and M. Jamshidi, "Trajectory tracking by multiple agents in formation with collision avoidance and connectivity assurance," *IEEE Syst. J.*, vol. 12, no. 3, pp. 2449–2460, Sep. 2018.
- [25] C. K. Verginis, A. Nikou, and D. V. Dimarogonas, "Robust formation control in SE(3) for tree-graph structures with prescribed transient and steady state performance," *Automatica*, vol. 103, pp. 538–548, May 2019.
- [26] F. Mehdifar, C. P. Bechlioulis, F. Hashemzadeh, and M. Baradarannia, "Prescribed performance distance-based formation control of multi-agent systems," *Automatica*, vol. 119, no. 6, 2020, Art. no. 109086.
- [27] C. P. Bechlioulis and G. A. Rovithakis, "Robust adaptive control of feedback linearizable MIMO nonlinear systems with prescribed performance," *IEEE Trans. Autom. Control*, vol. 53, no. 9, pp. 2090–2099, Oct. 2008.
- [28] Y. Li, X. Shao, and S. Tong, "Adaptive fuzzy prescribed performance control of Nontriangular structure nonlinear systems," *IEEE Trans. Fuzzy Syst.*, vol. 28, no. 10, pp. 2416–2426, Oct. 2020.
- [29] C. P. Bechlioulis and G. A. Rovithakis, "Decentralized robust synchronization of unknown high order nonlinear multi-agent systems with prescribed transient and steady state performance," *IEEE Trans. Autom. Control*, vol. 62, no. 1, pp. 123–134, Jan. 2017.

- [30] Z. Zuo, Q.-L. Han, B. Ning, X. Ge, and X.-M. Zhang, "An overview of recent advances in fixed-time cooperative control of multiagent systems," *IEEE Trans. Ind. Informat.*, vol. 14, no. 6, pp. 2322–2334, Jun. 2018.
- [31] Y. Li, K. Li, and S. Tong, "Finite-time adaptive fuzzy output feedback dynamic surface control for MIMO Nonstrict feedback systems," *IEEE Trans. Fuzzy Syst.*, vol. 27, no. 1, pp. 96–110, Jan. 2019.
- [32] A. Polyakov, "Nonlinear feedback design for fixed-time stabilization of linear control systems," *IEEE Trans. Autom. Control*, vol. 57, no. 8, pp. 2106–2110, Aug. 2012.
- [33] B. Ning, J. Jin, and J. Zheng, "Fixed-time consensus for multi-agent systems with discontinuous inherent dynamics over switching topology," *Int. J. Syst. Sci.*, vol. 48, no. 10, pp. 2023–2032, 2017.
- [34] H. Hong, W. Yu, X. Yu, G. Wen, and A. Alsaedi, "Fixed-time connectivity-preserving distributed average tracking for Multiagent systems," *IEEE Trans. Circuits Syst. II, Exp. Briefs*, vol. 64, no. 10, pp. 1192–1196, Oct. 2017.
- [35] Z. Zuo, "Nonsingular fixed-time consensus tracking for second-order multi-agent networks," *Automatica*, vol. 54, pp. 305–309, Apr. 2015.
- [36] K. P. Tee, S. S. Ge, and E. H. Tay, "Barrier Lyapunov functions for the control of output-constrained nonlinear systems," *Automatica*, vol. 45, no. 4, pp. 918–927, 2009.
- [37] X. Jin, "Fault tolerant finite-time leader-follower formation control for autonomous surface vessels with LOS range and angle constraints," *Automatica*, vol. 68, pp. 228–236, Jun. 2016.
- [38] X. Jin, "Adaptive fixed-time control for MIMO nonlinear systems with asymmetric output constraints using universal barrier functions," *IEEE Trans. Autom. Control.*, vol. 64, no. 7, pp. 3046–3053, Jul. 2019.
- Trans. Autom. Control, vol. 64, no. 7, pp. 3046–3053, Jul. 2019.

 [39] S.-L. Dai, S. He, H. Cai, and C. Yang, "Adaptive leader–follower formation control of underactuated surface vehicles with guaranteed performance," *IEEE Trans. Syst., Man, Cybern., Syst.*, vol. 52, no. 3, pp. 1997–2008, Mar. 2022.
- [40] T. Li, R. Zhao, C. L. P. Chen, L. Fang, and C. Liu, "Finite-time formation control of under-actuated ships using nonlinear sliding mode control," *IEEE Trans. Cybern.*, vol. 48, no. 11, pp. 3243–3253, Nov. 2018.
- [41] B. Tian, H. Lu, Z. Zuo, and W. Yang, "Fixed-time leader-follower output feedback consensus for second-order multiagent systems," *IEEE Trans. Cybern.*, vol. 49, no. 4, pp. 1545–1550, Apr. 2019.
- Cybern., vol. 49, no. 4, pp. 1545–1550, Apr. 2019.
 [42] B. Ning, Q.-L. Han, and Z. Zuo, "Practical fixed-time consensus for integrator-type multi-agent systems: A time base generator approach," Automatica, vol. 105, pp. 406–414. May 2019.
- Automatica, vol. 105, pp. 406–414, May 2019.
 [43] L. Asimow and B. Roth, "The rigidity of graphs, II," J. Math. Anal. Appl., vol. 68, no. 1, pp. 171–190, 1979.
- [44] B. Anderson, C. Yu, B. Fidan, and J. Hendrickx, "Rigid graph control architectures for autonomous formations," *IEEE Control Syst. Mag.*, vol. 28, no. 6, pp. 48–63, Dec. 2008.
- [45] B. Hendrickson, "Conditions for unique graph realizations," SIAM J. Comput., vol. 21, no. 1, pp. 65–84, 1992.
- [46] I. Izmestiev, Infinitesimal Rigidity of Frameworks and Surfaces, Kyushu Univ., Fukuoka, Japan, 2009.
- [47] J. Aspnes et al., "A theory of network localization," *IEEE Trans. Mobile Comput.*, vol. 5, no. 12, pp. 1663–1678, Dec. 2006.
- [48] X. Cai and M. de Queiroz, "Formation maneuvering and target interception for multi-agent systems via rigid graphs," *Asian J. Control*, vol. 17, no. 4, pp. 1174–1186, 2015.
- [49] X. Cai and M. de Queiroz, "Adaptive rigidity-based formation control for Multirobotic vehicles with dynamics," *IEEE Trans. Control Syst. Technol.*, vol. 23, no. 1, pp. 389–396, Jan. 2015.
- [50] Z. Zuo, B. Tian, M. Defoort, and Z. Ding, "Fixed-time consensus tracking for multiagent systems with high-order integrator dynamics," *IEEE Trans. Autom. Control*, vol. 63, no. 2, pp. 563–570, Feb. 2018.



Ke Lu (Graduate Student Member, IEEE) received the B.E. degree in material engineering from Nanjing Forestry University, Nanjing, China, in 2015, and the M.Sc. degree in mechanical and automation engineering from the Chinese University of Hong Kong, Hong Kong, in 2017. He is currently pursuing the Ph.D. degree in control science and engineering with the School of Automation Science and Engineering, South China University of Technology, Guangzhou, China.

His current research interests include adaptive

control system and coordination and control of multiagent systems.



Shi-Lu Dai (Member, IEEE) received the B.Eng. degree in thermal engineering and the M.Eng. and Ph.D. degrees in control science and engineering from Northeastern University, Shenyang, China, in 2002, 2006, and 2010, respectively.

He was a visiting student with the Department of Electrical and Computer Engineering, National University of Singapore, Singapore, from November 2007 to November 2009, and a Visiting Scholar with the Department of Electrical Engineering, University of Notre Dame, Notre Dame, IN, USA, from

October 2015 to October 2016. He has been with the School of Automation Science and Engineering, South China University of Technology, Guangzhou, China, since 2010, where he is currently a Professor. His current research interests include adaptive and learning control, cooperative control, and autonomous vehicles.



Xu Jin (Member, IEEE) received the Bachelor of Engineering degree (First Hons.) in electrical and computer engineering from the National University of Singapore, Singapore, in 2013, the Master of Applied Science degree in electrical and computer engineering from the University of Toronto, Toronto, ON, Canada, in 2015, the Master of Science degree in mathematics and the Doctor of Philosophy degree in aerospace engineering from the Georgia Institute of Technology, Atlanta, GA, USA, in 2018 and 2019, respectively.

He is currently an Assistant Professor with the Department of Mechanical and Aerospace Engineering, University of Kentucky, Lexington, KY, USA. He has authored/coauthored over 50 peer-reviewed journal and conference papers. His current research interests include adaptive and iterative learning control, fault-tolerant control, nonlinear systems control, with applications to intelligent vehicles, autonomous robots, and multiagent systems.

Dr. Jin has been a reviewer for over 20 journals in areas of control systems and applications.